(Ga,Mn)As grown on (311) GaAs substrates: Modified Mn incorporation and magnetic anisotropies

K. Y. Wang,[1] K. W. Edmonds,[1] L. X. Zhao,[1] M. Sawicki,[2] R. P. Campion,[1] B. L. Gallagher,[1] and C. T. Foxon[1]
[1]*School of Physics and Astronomy, University of Nottingham, Nottingham NG7 2RD, United Kingdom*
[2]*Institute of Physics, Polish Academy of Sciences, and ERATO Semiconductor Spintronics Project, PL 02-668 Warszawa, Poland*
(Received 21 February 2005; published 15 September 2005)

We report the results of a detailed study of the structural, magnetic, and magnetotransport properties of as-grown and annealed $Ga_{0.91}Mn_{0.09}As$ thin films grown on (311)*A* and (311)*B* GaAs substrates. The high Curie temperature and hole density of the (311)*B* material are comparable to those of GaMnAs grown on (001) GaAs under the same growth conditions, while they are much lower for the (311)*A* material. We find evidence that Mn incorporation is more efficient for (311)*B* than for (001) and significantly less efficient for (311)*A* which is consistent with the bonding on these surfaces. This indicates that growth on (311*B*) may be a route to increased Curie temperatures in GaMnAs. A biaxial magnetic anisotropy is observed for the (311) material with easy axes along the [010] and [001] out-of-plane directions. An additional uniaxial in-plane anisotropy is also observed with the easy axis along $[01\bar{1}]$ for the (311)*A* material, and along $[\bar{2}33]$ for the (311)*B* material. This observation may be of importance for the resolution of the outstanding problem of the origin of uniaxial anisotropy in (001) GaMnAs.

DOI: 10.1103/PhysRevB.72.115207 PACS number(s): 75.70.Ak, 75.47.−m, 75.50.Pp

INTRODUCTION

The ferromagnetic semiconductor GaMnAs has attracted considerable interest, mainly because of the prospect of developing devices which combine information processing and storage functionalities in one material.[1,2] When Mn atoms occupy the Ga site they act as acceptors. The Curie temperature T_C of GaMnAs is strongly dependent on both the effective Mn concentration x_{eff} and the hole density p, varying roughly as $x_{\mathrm{eff}}p^{1/3}$.[3] GaMnAs films grown on GaAs (001) substrates by low-temperature molecular beam epitaxy are under compressive strain, which for sufficiently high hole density leads to an in-plane magnetic easy axes.[4] The magnetic properties of GaMnAs as-grown samples can be phenomenologically described by a single domain model considering coexisting in-plane biaxial and uniaxial anisotropies.[5–7]

Growth of GaMnAs on higher index substrates has attracted much less attention. This is surprising given that this may offer a new degree of freedom for engineering magnetic anisotropies and maximizing incorporation of magnetic impurities. There are reports of GaMnAs grown on (411)*A* GaAs,[8] and very recently, on (311)*A* GaAs.[9] In both cases, magnetotransport measurements gave evidence for magnetic easy axes aligned partially along the growth direction, in the (001) plane, although the film quality was rather low compared to GaMnAs grown on (001) GaAs. In this paper we report the results of a comparative study of the structural, magnetic, and magnetotransport properties of as-grown and annealed $Ga_{0.91}Mn_{0.09}As$ thin films grown on (311)*A* and (311)*B* GaAs substrates. We examine in detail the resulting magnetic anisotropies, and contrast these to the widely reported behavior of GaMnAs on (001) GaAs. We also investigate the differing efficiencies of Mn incorporation on these surfaces and the effect of this on the Curie temperatures obtained.

EXPERIMENT

50 nm thick $Ga_{0.91}Mn_{0.09}As$ films were grown on (311)*A* and (311)*B* substrates by low temperature molecular beam epitaxy under identical growth conditions to those used for (001) GaMnAs. The growth,[10] structural,[11] magnetic,[12] and magnetotransport[13] properties of the (001) GaMnAs layers are described in detail elsewhere. A 100 nm thick high-temperature GaAs layer, followed by a 50 nm thick low-temperature GaAs layer, were deposited prior to growth of the GaMnAs films. The nominal Mn concentration of 9% is obtained from the Ga/Mn flux ratio, as calibrated by secondary ion mass spectrometry measurements on 1 μm thick films grown on (001)GaAs. We note however that it may be substantially different for the (311) materials for which the efficiency of Mn incorporation may be significantly different from that for (001). Post-growth annealing was performed in air at 190 °C for around 100 hours, which is an established procedure for increasing the T_C of thin GaMnAs films.[14,15] The structural properties were measured by high resolution x-ray diffraction. To obtain accurate relaxed lattice parameters, the $\omega/2\theta$ curves obtained are compared with simulations using Philips X'Pert epitaxy software package of the PANalytical X'Pert XRD system. Standard hall bar structures were photolithographically fabricated for transport measurements, with the current direction along the $[\bar{2}33]$ axis. Magnetotransport measurements were performed, using low frequency ac techniques, in a cryomagnetic system, in which the magnetic field can be rotated *in-situ* along any direction relative to the sample axes. The magnetic properties of the layers were measured using a SQUID magnetometer, which has been custom designed to give very low trapped fields in the superconducting coil (<0.1 Oe) after a field sweep up to 1000 Oe.

 ©2005 The American Physical Society

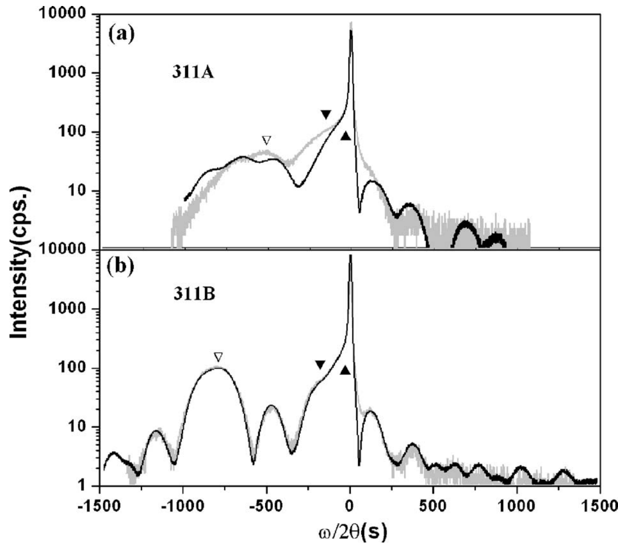

FIG. 1. $\omega/2\theta$ plots for (Ga,Mn)As grown on (311)A and (311)B GaAs. Features corresponding to the GaAs substrate (solid triangle) LT-GaAs buffer (solid down triangle) and GaMnAs layer (open down triangle) are marked. The gray curves are experimental data and the black curves are simulations.

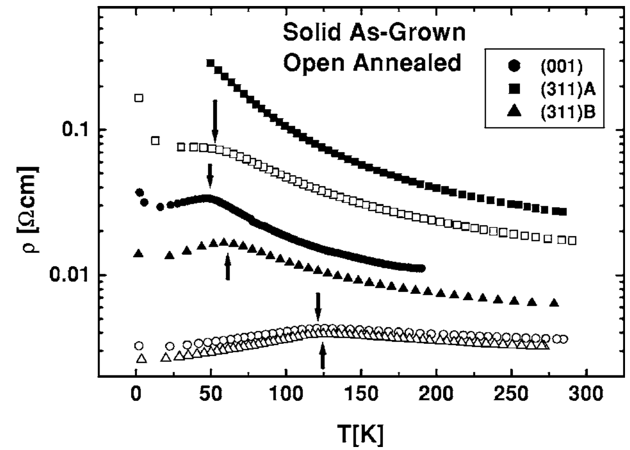

FIG. 2. Resistivity versus temperature for as-grown and annealed (Ga,Mn)As films grown under similar conditions on (001) (circles), (311)A (squares), and (311)B (triangles) GaAs substrates, where the peak temperature T_ρ are marked with arrows. The solid symbols are for as-grown samples, the open symbols are for annealed samples.

RESULTS AND DISCUSSION

Structure

Figure 1 shows experimental and simulated x-ray diffraction $2\theta/\omega$ plots for the as-grown, (311)A and B GaMnAs samples. Features corresponding to the GaAs substrate, the low-temperature GaAs buffer layer, and the GaMnAs layer are marked. The lattice constant in the LT-GaAs buffer layer is slightly expanded compared to the substrate, probably due to As_{Ga} defects. The GaMnAs peak is much broader for (311)A compared to (311)B indicating poorer structural quality, and it is at higher $2\theta/\omega$. The width of the GaMnAs peak for the (311)B film is similar to that of the (001) film, indicating comparable structural quality. The lattice constant obtained for (311)B samples is significantly larger than that for (311)A samples. Since the lattice constant in GaMnAs increases with increasing Mn concentration,[16] this indicates that less Mn has been incorporated in the (311)A case. As shown in Table I, the strain $\Delta a/a$ is the largest for 311B in these three samples, which indicates the most efficient Mn incorporation for 311B.

Magnetotransport

The resistivity (ρ) as a function of temperature (T) for the as-grown and post-annealed (311) GaMnAs films is shown in Fig. 2, together with data for a 50 nm (001) GaMnAs film grown under the same conditions. For (311B), the resistivity exhibits a clear peak at temperature T_ρ corresponding roughly to the onset of ferromagnetic ordering, as is typically observed in GaMnAs films on the metallic side of the metal-insulator transition (MIT).[16,17] On annealing, the resistivity decreases while T_ρ moves to higher temperatures. Both the resistivity and T_ρ are comparable to those obtained for the (001) sample. In contrast, the resistivity of the (311)A film is much higher. The film is on the insulator side of the MIT before annealing, and close to the transition after annealing. Room temperature Hall measurements show that all the samples are p type. Low temperature high field Hall measurements[17,18] give the hole densities listed in Table I for the (001) and (311)B samples. At low temperatures, the resistance is too high to accurately study the magnetotransport properties of (311)A samples. However, it can be clearly seen from Table I that the electrical and magnetic properties are better for the (311)B film than for the (311A) film, and that these properties improve on annealing of both films.

TABLE I. The strain $\Delta a/a$, hole density p, Curie temperature T_C, and saturation magnetization M_S at 5 K for 50 nm thick $Ga_{0.91}Mn_{0.09}As$ films grown on (001), (311)A, and (311)B GaAs substrates. Here a is the relaxed lattice constant of the GaMnAs epilayer and $\Delta a = a - a_0$, where a_0 is the lattice constant of the GaAs substrate.

	(001)	(001)ann	(311)A	(311)A_{ann}	(311)B	(311)B_{ann}
$\Delta a/a(\times 10^{-3})$	3.65		3.1		4.5	
$p\pm 0.3(\times 10^{20}\ cm^{-3})$	0.9	5.5		0.31	0.92	5.43
$T_C\pm 2$(K)	56	133	38	62	62	125
$M_S\pm 0.3(\mu_B/Mn)$	2.1	2.6	1.2	1.7	2.2	3.9

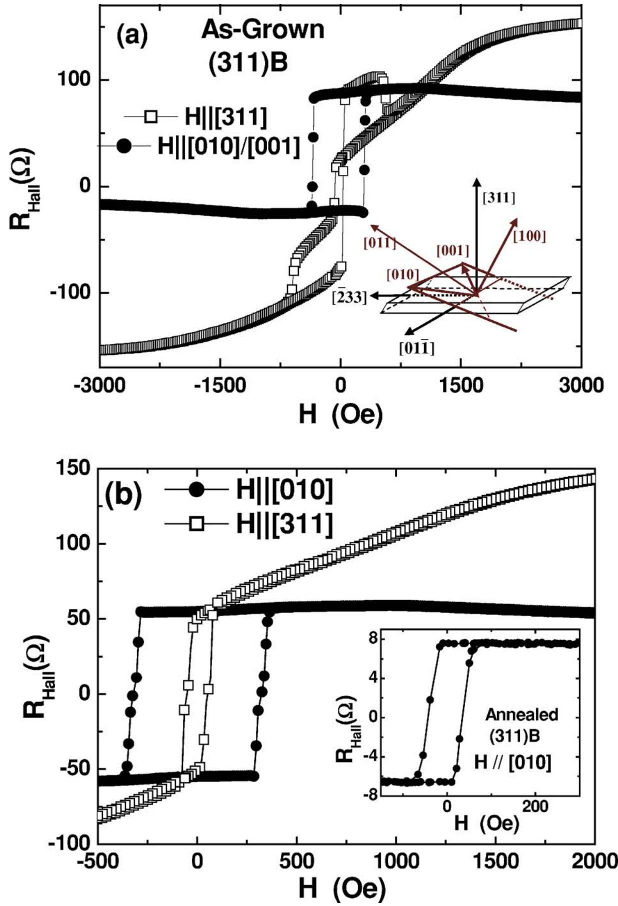

FIG. 3. (Color online) (a) Hall resistance, including planar Hall contribution, for as-grown (Ga,Mn)As on (311)*B* GaAs at 4 K, for magnetic field applied along the [311] (squares) and [010]/[001] (circles) directions. Inset of (a) the 3D schematic diagram for 311 material, (b) extracted anomalous Hall resistance for the data in (a); inset of (b). Hall resistance for field along the [010]/[001] direction at 4 K for annealed (Ga,Mn)As film on (311)*B* GaAs.

For the (311)*B* sample, Hall measurements show a clear, albeit complicated, Hall response. The measured Hall resistance, R_{Hall}, versus magnetic field applied along the [311] and [010]/[001] directions are shown in Fig. 3(a) for the as-grown (311)*B* sample. The three-dimensional (3D) schematic diagram for the 311 material is shown in the inset of Fig. 3(a). We note here, that one can unambiguously distinguish the (233) and (011) planes. Looking from the top, the upright plane is the (011) plane and the cutting edge plane is the (233) plane. [010]/[001] directions are tilted 17.5° out of the film plane. Along [010]/[001] R_{Hall} has a square loop which is offset from zero, followed by a slow decrease; while for the [311] directions the loop is even more complicated, showing a crossover of increasing and decreasing field sweeps. The measured R_{Hall} is a superposition of two distinct contributions. First the anomalous Hall contribution which is given by $R_A=\alpha_A\rho^{\gamma}M_z$, where α_A is the anomalous Hall coefficient, and M_z is the perpendicular component of the magnetization. For GaMnAs in the metallic regime $\gamma\sim 2$.[18] The second contribution is from the so-called Planar Hall effect, which arises due to a difference in conductivity for current parallel and perpendicular to the magnetization direction. This is approximately given by $R_P=\alpha_P\sin(2\theta)$, where θ is the angle between magnetization and current directions. The large planar Hall contribution observed when the field is applied along [311] indicates that θ varies during the magnetization reversal.

The planar Hall effect is not a true Hall effect, i.e., is not antisymmetric in the magnetic field, so the anomalous Hall resistance can be extracted from the measured R_{Hall} using the expressions

$$R_A(\downarrow)=[R_{\mathrm{Hall}}(\downarrow,+)-R_{\mathrm{Hall}}(\uparrow,-)]/2$$

and

$$R_A(\uparrow)=[R_{\mathrm{Hall}}(\uparrow,+)-R_{\mathrm{Hall}}(\downarrow,-)]/2,$$

where ↑, ↓, +, − represent increasing, decreasing, positive, and negative external magnetic fields, respectively. The extracted R_A for field along the [311] and [010]/[001] directions is shown in Fig. 3(b). For both directions, a sharp switch between ±60Ω is observed at low fields. At higher fields, R_A (and thus M_z) increases slowly and reversibly for the [311] direction, which is characteristic of rotation away from an easy magnetic axis, while for the [010]/[001] directions R_A remains almost constant above the switching field of ~300 Oe. This indicates that the magnetization is saturated along this direction (note that the small decrease in R_{Hall} at higher fields is due to its dependence on ρ, which shows an isotropic negative magnetoresistance as is commonly observed in (001) GaMnAs.[16] Therefore, the Hall resistance data indicate that the (311)*B* film has easy axes along the [010] and [001] directions, which are tilted out-of-plane. Square Hall traces are also observed for the annealed (311)*B* film for field parallel to the [010]/[001] directions, as shown in the inset of Fig. 3(b). Similar anisotropies have been reported previously for GaMnAs grown on (411)*A* GaAs,[8] and have been ascribed to the strain-induced anisotropy of the GaMnAs valence band.

Magnetometry

SQUID hysteresis loops for the as-grown and annealed (311)*A* and *B* samples at 5 K are shown in Fig. 4, for magnetic fields applied along the orthogonal [01$\bar{1}$], [$\bar{2}$33], and [311] axes (it proved impossible to perform reliable magnetometry measurements with the applied field along the ⟨100⟩ directions in the SQUID magnetometer). The diamagnetic contribution from the substrate has been subtracted. The measured magnetization is normalized to the nominal Mn concentration. The magnetization is larger for (311)*B* than for (311)*A*, again indicating that a larger amount of the incident Mn is incorporated substitutionally in the former case. The magnetization increases on annealing, as is typically observed in (001) GaMnAs films. As shown in Table I, for the annealed (311)*B* film the measured magnetic moment per Mn is $(3.9\pm0.3)\mu_B$, which is even much larger than the value of $(2.6\pm0.3)\mu_B$ observed for the (001) material. This is again consistent with a larger fraction of the nominal Mn concentration of 9% being incorporated substitutionally in the

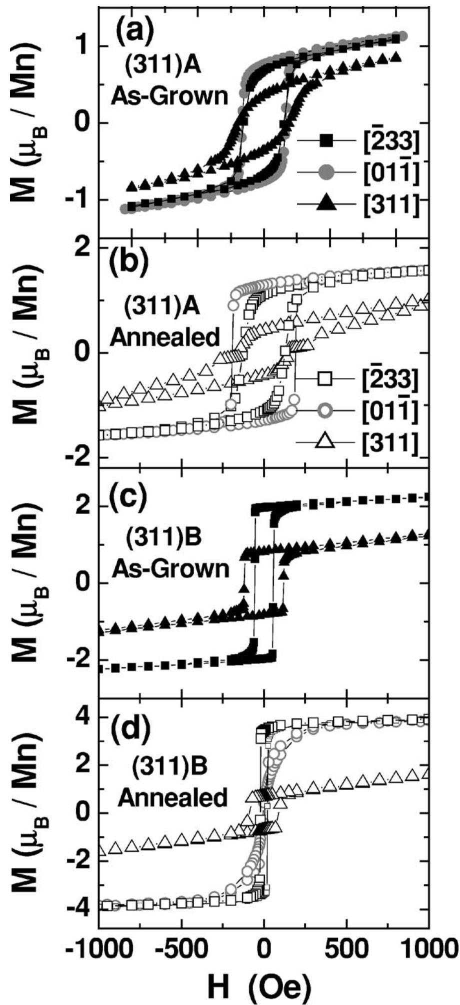

FIG. 4. Magnetization hysteresis loops at 5 K for three orthogonal directions [01$\bar{1}$] (circles), [$\bar{2}$33] (squares), and [311] (triangles), for (a) as-grown (Ga,Mn)As on (311)*A* GaAs; (b) annealed (Ga,Mn)As on (311)*A* GaAs; (c) as-grown (Ga,Mn)As on (311)*B* GaAs (measurement along [01$\bar{1}$] not shown); (d) annealed (Ga,Mn)As on (311)*B* GaAs. The diamagnetic contribution from the substrate has been subtracted in each case.

(311)*B* film than in (001) film. Since the surface As atoms are twofold coordinated on the (311)*A* surface and threefold coordinated on the (311)*B* surface, this indicates that Mn is incorporated more readily at a single-dangling bond site. A similar situation is also observed in Si-doping of (311)GaAs, where incorporation on As and Ga sites is favored for growth on *A* and *B* surfaces, respectively. This has been ascribed to a stronger bonding to the substrate of adatoms at double-dangling bond sites, so that breaking of the weaker single-dangling bonds is the limiting impurity incorporation process.[19]

For all four (311) samples and for all three orientations, significant hysteresis is observed, with larger remnant magnetization M_R along the in-plane orientations than along the perpendicular [311] direction. The angles between the [01$\bar{1}$], [$\bar{2}$33], and [311] axes and the [010]/[001] axes are, respectively, 45°, 50.2°, and 72.5°. Therefore, if the measured M_R represents the projection of the magnetization which is oriented along the easy [010]/[001] axes [as suggested by the Hall measurements on the (311)*B* film], we expect the M_R along [01$\bar{1}$], [$\bar{2}$33], and [311] to have the ratio cos(45°): cos(50.2°): cos(72.5°). This ratio is observed almost exactly for the as-grown (311)*A* sample, and approximately for the annealed (311)*A* and as-grown (311)*B* samples, although with a larger in-plane moment in the latter two. However, for the annealed (311)*B* sample, the M_R along [$\bar{2}$33] is by far the largest, with a pronounced anisotropy between this and the [01$\bar{1}$] direction. These measurements indicate that the films also possess a uniaxial magnetic anisotropy which favors in-plane orientation of the magnetization, and the ratio of the strength of the uniaxial to biaxial anisotropy increases on going from as-grown (311)*A*, to annealed (311)*A*, to as-grown (311)*B*, to annealed (311)*B*, i.e., following the order of increasing T_C.

To obtain more detailed information about the magnetic anisotropy and its temperature dependence in the films, the temperature dependence of the remnant magnetization is studied. First, the sample is cooled through T_C down to 5 K under an external field of 1000 Oe applied along the measurement axis. Then, the field is removed, and the projection of the remnant magnetization along the measurement axis is recorded as a function of increasing temperature. Since the trapped fields in the superconducting coil are very low, the sample magnetization rotates to the nearest magnetic easy direction set only by the torques exerted by internal anisotropy fields. These measurements were performed sequentially for the orthogonal [01$\bar{1}$], [$\bar{2}$33], and [311] orientations.

The temperature dependence of the M_R for the as-grown and annealed (311)*A* and (311)*B* films are shown in Fig. 5. The Curie temperatures obtained from this procedure are in agreement with those obtained from transport measurements, shown in Table I. The measured remnant magnetization projections indicate the presence of both in-plane uniaxial and [001]/[010] biaxial anisotropies, consistent with the hysteresis measurements. With increasing temperature, the uniaxial anisotropy becomes dominant. The uniaxial easy axis is along [01$\bar{1}$] in the (311)*A* case and along [$\bar{2}$33] in the (311)*B* case, both before and after annealing.

It is useful to compare the magnetic anisotropy of the (311) films to previously reported behavior for (001) GaMnAs under compressive strain.[5–7,12,13,20,21] In such films, biaxial anisotropy with in-plane [100] and [010] easy axes typically dominates at low temperatures, giving way to a uniaxial anisotropy between in-plane [110] and [1$\bar{1}$0] directions at high temperatures. Low temperature annealing tends to enhance the in-plane uniaxial anisotropy relative to the biaxial,[20] and causes a rotation of the uniaxial easy axis from the [1$\bar{1}$0] direction to the [110].[12] The origin of the symmetry breaking between [110] and [1$\bar{1}$0] in (001) GaMnAs is presently unknown.

While a uniaxial anisotropy is expected in the present case since the [01$\bar{1}$] and [$\bar{2}$33] directions are not symmetric, the different orientation of the uniaxial easy axis is somewhat surprising since the structures of (311)*A* and (311)*B*

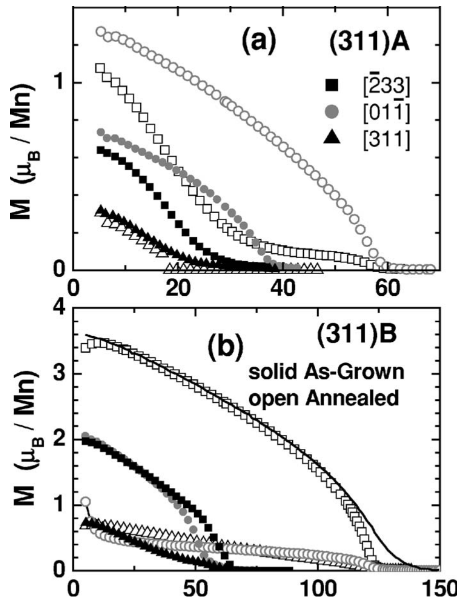

FIG. 5. Remnant magnetization along the $[01\bar{1}]$ (circles), $[\bar{2}33]$ (squares), and [311] (triangles) axes versus increasing temperature, after cooling from above T_C under a 1000 Oe field, for (a) as-grown and annealed (Ga,Mn)As on (311)*A* GaAs and (b) as-grown and annealed (Ga,Mn)As on (311)*B* GaAs. Measurements on as-grown and annealed films are denoted by full and open symbols, respectively. The solid line in (b) is the magnetization along $[\bar{2}33]$ under a 1000 Oe field, where the diamagnetic contribution from the substrate has been subtracted.

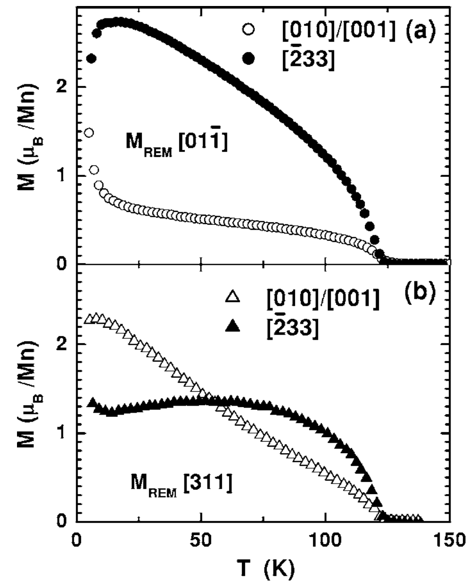

FIG. 6. Estimated (see text) magnetization oriented along [010]/[001] and $[\bar{2}33]$ orientations versus increasing temperature after cooling under an external field applied along (a) $[01\bar{1}]$ and (b) [311] axes, for the annealed (Ga,Mn)As film on (311)*B* GaAs.

differ only at the surface and interface layers. It has been suggested for (001) GaMnAs (Ref. 21) that the uniaxial anisotropy results from an anisotropic incorporation of Mn during growth. However, for the 311*A* and 311*B* surfaces, similar (8×1) surface reconstruction along $[01\bar{1}]$ direction has been observed for (311)*A* and (311)*B* GaAs samples[22,23] and the Ga bonds on both surfaces align along the $[0\bar{1}1]$ direction. Therefore, an anisotropic incorporation is unlikely to be responsible for the difference in the uniaxial anisotropy between (311)*A* and (311)*B*. We therefore attribute the uniaxial anisotropy rotation to the higher incorporation on the *B* surface, leading to a higher hole density, since the direction of the uniaxial easy axis has been shown to be hole-density dependent in the case of (001) GaMnAs. However, we cannot rule out that the higher concentration of local moments also plays a role.

The temperature-dependent magnetization under a 1000 Oe external field applied along the $[\bar{2}33]$ direction for the annealed (311)*B* sample is also shown in Fig. 5. After subtracting the diamagnetic background from the substrate, this is almost identical to the remnant measurement. This indicates that, after field cooling to align the magnetization along the $[\bar{2}33]$ direction, the M_R remains fixed along this direction on warming. Differences are only observed close to T_C, due to the paramagnetic response of the GaMnAs layer under magnetic field, and at very low temperatures, where comparison of the M_R traces for the three orientations appears to suggest that the easy axis rotates away from $[\bar{2}33]$ and towards the [010]/[001] directions. However, applying a field along the $[01\bar{1}]$ or [311] directions results in a net M_R along these directions, indicating that the magnetization does not rotate into the $[\bar{2}33]$ easy axis on sweeping the external field to zero. From this we conclude that the M_R is partially oriented along the [010] and [001] axes after applying a field along $[01\bar{1}]$ or [311]. Assuming that the measured M_R along these two directions corresponds to the projection of the [010] and [001] magnetization, while the magnetization which is not detected is aligned with the $[\bar{2}33]$ direction, we obtain the components of the magnetization along the [010]/[001] and $[\bar{2}33]$ directions after field cooling along $[01\bar{1}]$ or [311] as shown in Fig. 6. Quite different results are obtained for $[01\bar{1}]$ and [311], with the latter giving rise to a larger magnetization along the [010]/[001] directions. This demonstrates that the magnetic state may be strongly history dependent in (311) GaMnAs, with large energy barriers separating uniaxial in-plane and biaxial out-of-plane easy axes.

SUMMARY

We have studied the structural, magnetotransport, and magnetic properties of $Ga_{0.91}Mn_{0.09}As$ thin films grown on (311)*A* and (311)*B* GaAs substrates. The larger lattice constant, Curie temperature, conductivity, and saturation magnetization observed for the (311)*B* sample are all evidence that a higher fraction of incident Mn is incorporated substitutionally at Ga sites for growth on (311)*B* than on (311)*A*. For both (311)*A* and (311)*B*, a factor of 2 increase in T_C is obtained on annealing, indicating that Mn is also incorporated on interstitial sites in both cases.[24] Despite evidence for higher Mn incorporation for (311)*B* than for (001) the mate-

rials show comparable T_C, hole density and conductivity suggesting that the concentration of compensating defects such as As_{Ga} may also be larger. Therefore, with further optimization growth on (311)B may be a route to higher temperature ferromagnetism in GaMnAs.

The (311) GaMnAs films show a complex and interesting magnetic anisotropy, with competition between out-of-plane biaxial [010]/[001] easy axes, and in-plane uniaxial easy axis. With increasing temperature, the in-plane easy axis becomes dominant. Low temperature annealing strongly enhances the in-plane uniaxial anisotropy relative to the biaxial. Similar behavior has also been observed in (001) material. Moreover, the in-plane easy axis is along the $[01\bar{1}]$ direction for the (311)A sample and along the $[\bar{2}33]$ direction for the (311)B sample. While the origin of the easy axis rotation is not presently known, this observation may hold important clues regarding the origin of the in-plane uniaxial anisotropy observed in (001) GaMnAs.

ACKNOWLEDGMENTS

The project was funded by EPSRC (GR/S81407/01) and EU FENIKS (G5RD-CT-2001-0535). The authors gratefully acknowledge useful discussions with T. Dietl, C. Staddon, and M. Henini. The authors thank Jaz Chauhan and Dave Taylor for processing of the Hall bars.

[1] T. Dietl, H. Ohno, F. Matsukura, J. Cibert, and D. Ferrand, Science **287**, 1019 (2000).
[2] S. A. Wolf, D. D. Awschalom, R. A. Buhrman, J. M. Daughton, S. von Molnaar, M. L. Roukes, A. Y. Chtchelkanova, and D. M. Treger, Science **294**, 1488 (2001).
[3] T. Dietl, H. Ohno, and F. Matsukura, Phys. Rev. B **63**, 195205 (2001).
[4] H. Ohno, F. Matsukura, A. Shen, Y. Sugawara, A. Oiwa, A. Endo, S. Katsumoto, and Y. Iye, in *Proceedings of the 23rd International Conference on the Physics of Semiconductors, Berlin 1996*, edited by M. Scheffler and R. Zimmermann (World Scientific, Singapore, 1996), p. 405.
[5] K. Y. Wang, M. Sawicki, K. W. Edmonds, R. P. Campion, S. Maat, C. T. Foxon, B. L. Gallagher, and T. Dietl, cond-mat/0507187 (unpublished).
[6] U. Welp, V. K. Vlasko-Vlasov, X. Liu, J. K. Furdyna, and T. Wojtowicz, Phys. Rev. Lett. **90**, 167206 (2003).
[7] H. X. Tang, R. K. Kawakami, D. D. Awschalom, and M. L. Roukes, Phys. Rev. Lett. **90**, 107201 (2003).
[8] T. Omiya, F. Matsukura, A. Shen, Y. Ohno, and H. Ohno, Physica E (Amsterdam) **10**, 206 (2001).
[9] M. Reinwald, U. Wurstbauer, M. Doppe, W. Kipferl, K. Wagenhuber, H.-P. Tranitz, D. Weiss, and W. Wegscheider, J. Cryst. Growth **278**, 690 (2005).
[10] R. P. Campion, K. W. Edmonds, L. X. Zhao, K. Y. Wang, C. T. Foxon, B. L. Gallagher, and C. R. Staddon, J. Cryst. Growth **247**, 42 (2003).
[11] L. X. Zhao, C. R. Staddon, K. Y. Wang, K. W. Edmonds, R. P. Campion, B. L. Gallagher, and C. T. Foxon, Appl. Phys. Lett. **86**, 071902 (2005).
[12] M. Sawicki, K. Y. Wang, K. W. Edmonds, R. P. Campion, C. R. Staddon, N. R. S. Farley, C. T. Foxon, E. Papis, E. Kamińska, A. Pitrowska, T. Dietl, and B. L. Gallagher, Phys. Rev. B **71**, 121302(R) (2005).
[13] K. Y. Wang, K. W. Edmonds, R. P. Campion, L. X. Zhao, C. T. Foxon, and B. L. Gallagher, Phys. Rev. B **72**, 085201 (2005).
[14] T. Hayashi, Y. Hashimoto, S. Katsumoto, and Y. Iye, Appl. Phys. Lett. **78**, 1691 (2001).
[15] K. W. Edmonds, K. Y. Wang, R. P. Campion, A. C. Neumann, N. R. S. Farley, B. L. Gallagher, and C. T. Foxon, Appl. Phys. Lett. **81**, 4991 (2002).
[16] F. Matsukura, H. Ohno, A. Shen, and Y. Sugawara, Phys. Rev. B **57**, R2037 (1998).
[17] K. W. Edmonds, K. Y. Wang, R. P. Campion, A. C. Neumann, C. T. Foxon, B. L. Gallagher, and P. C. Main, Appl. Phys. Lett. **81**, 3010 (2002).
[18] K. W. Edmonds, R. P. Campion, K. Y. Wang, A. C. Neumann, B. L. Gallagher, C. T. Foxon, and P. C. Main, J. Appl. Phys. **93**, 6787 (2003).
[19] W. I. Wang, R. F. Marks, and L. Vina, J. Appl. Phys. **59**, 937 (1986).
[20] H. Kato, K. Hamaya, T. Taniyama, Y. Kitamoto, and H. Munekata, Jpn. J. Appl. Phys., Part 2 **43**, L904 (2004).
[21] U. Welp, V. K. Vlasko-Vlasov, A. Menzen, H. D. You, X. Liu, J. K. Furdyna, and T. Wojtowicz, Appl. Phys. Lett. **85**, 260 (2004).
[22] Z. M. Wang, V. R. Yazdanpanah, J. L. Shultz, and G. J. Salamo, Appl. Phys. Lett. **81**, 2965 (2002).
[23] M. Wassermeier, J. Sudijono, M. D. Johnson, K. T. Leung, B. G. Orr, L. Daweritz, and K. Ploog, Phys. Rev. B **51**, 14721 (1995).
[24] K. M. Yu, W. Walukiewicz, T. Wojtowicz, I. Kuryliszn, X. Liu, S. Sasaki, and J. K. Furdyna, Phys. Rev. B **65**, 201303(R) (2002).